



# Stem CH<sub>4</sub> and N<sub>2</sub>O fluxes of *Fraxinus excelsior* and *Populus alba* trees along a flooding gradient

Erwin Moldaschl · Barbara Kitzler · Katerina Machacova · Thomas Schindler · Andreas Schindlbacher

Received: 29 April 2020 / Accepted: 20 December 2020 / Published online: 25 January 2021  
© The Author(s), under exclusive licence to Springer Nature Switzerland AG part of Springer Nature 2021

## Abstract

**Aims** Methane (CH<sub>4</sub>) and nitrous oxide (N<sub>2</sub>O) fluxes from tree stems are still poorly quantified in temperate floodplain forests.

**Methods** Methane and N<sub>2</sub>O fluxes were repeatedly measured at 0.3, 1.6 and 3.6 m stem height at three sites along a landscape gradient ranging from non-flooded to frequently flooded forest sites. The non-flooded forest was dominated by *Fraxinus excelsior* and the infrequently and frequently flooded sites by *Populus alba*.

**Results** Stem surfaces were net CH<sub>4</sub> and N<sub>2</sub>O sources at all sites. The CH<sub>4</sub> source strength increased towards the wetter sites (non-flooded 2.51±12.71, infrequently-flooded 5.2±17.26, and frequently-flooded 11.15 ±24.04 μg-C-m<sup>-2</sup> h<sup>-1</sup>), but flooding had no immanent effects on CH<sub>4</sub> and N<sub>2</sub>O fluxes. Methane fluxes from poplar stems were highest at the stem base (0.3 m) and decreased with increasing measurement height. Methane fluxes from ash stems were lowest at the stem base

and gradually increased until 3.6 m height. Nitrous oxide fluxes were low and did not show clear spatial patterns. The presence of mosses had no significant effects on CH<sub>4</sub> and N<sub>2</sub>O fluxes.

**Conclusions** Stem fluxes were small when compared to the corresponding soil fluxes at the non-flooded and infrequently flooded site, but significantly reduced the soil CH<sub>4</sub> sink capacity at the frequently-flooded site. Methane flux strongly varied between 0.3 and 3.6 m stem height and showed distinctive tree species specific patterns. Our results therefore suggest that measuring at more than a single location near the stem base is inevitable to obtain any reliable CH<sub>4</sub> or N<sub>2</sub>O flux estimate of a whole tree stem.

**Keywords** Stem GHG emissions · Stem height · Flooding · Temperate floodplain forest · CH<sub>4</sub> · N<sub>2</sub>O · *Fraxinus excelsior* · *Populus alba*

Responsible Editor: Paul Bodelier

E. Moldaschl (✉) · B. Kitzler · A. Schindlbacher  
Federal Research and Training Centre for Forests, Natural Hazards and Landscape, Seckendorff-Gudent-Weg 8, 1131 Vienna, Austria  
e-mail: erwin.moldaschl@boku.ac.at

K. Machacova  
Global Change Research Institute of the Czech Academy of Sciences, Belidla 4a, CZ-60300 Brno, Czech Republic

T. Schindler  
Institute of Ecology and Earth Science, University of Tartu, Vanemuise 46, 51003 Tartu, Estonia

## Introduction

Tree stem surfaces can be important sources and/or sinks of the greenhouse gases (GHG) methane (CH<sub>4</sub>) and nitrous oxide (N<sub>2</sub>O). The magnitude of stem GHG fluxes and their contribution to the total forest GHG flux show high spatial and temporal variability on different scales and studies assessing stem GHG fluxes in situ are still scarce. Accordingly, the integration of stem GHG fluxes into forest GHG balance remains challenging (Lenhart et al. 2018; Barba et al. 2019; Covey and Megonigal 2019).

Particularly high stem emissions of CH<sub>4</sub> were observed in lowland tropical wetland forests, contributing up to more than 80% of the total ecosystem emissions (Pangala et al. 2017). Furthermore, under more moderate climate conditions, trees growing on water-logged soils typically show higher stem CH<sub>4</sub> emissions than under well-drained non-flooded conditions (Gauci et al. 2010; Pitz et al. 2018; Covey and Megonigal 2019). Water logging of forest soils causes anaerobic soil conditions, which is mandatory for microbial methanogenesis (Topp and Pattey 1997; Smith et al. 2018). A portion of the produced CH<sub>4</sub> can be transported through the plant and released via the stem surface into the atmosphere (Rusch and Renneberg 1998). Particularly in riparian forests, which are characterized by periods of flooding and soil water saturation, stem CH<sub>4</sub> emissions could offset the typically observed soil CH<sub>4</sub> uptake (Pitz and Megonigal 2017). Therefore, riparian ecosystems, such as the floodplain forests of the major temperate river basins, covering ~2,000,000 ha globally (Tockner and Stanford 2002), still represent a potential source of uncertainty in regional, national or global GHG-assessments (IPCC 2013).

The changing water tables, surface flooding, and periodic sediment deposition can turn floodplain forests into potential “hot spots” for nitrogen (N) cycling (Shrestha et al. 2012; Butterbach-Bahl et al. 2013; Krause et al. 2017). High soil N availability and the periodic alterations in soil water content can trigger denitrification processes and N<sub>2</sub>O production and release in soils (IPCC 2013; Kandel et al. 2018). Accordingly, tree stems in riparian ecosystems could provide pathways for soil-produced N<sub>2</sub>O (Machacova et al. 2013; Schindler et al. 2020). In non-flooded forests, tree stems were found to contribute approximately 1–10% of the total ecosystem N<sub>2</sub>O efflux (Díaz-Pinés et al. 2016; Machacova et al. 2016; Wen et al. 2017; Machacova et al. 2019). To our knowledge, no stem N<sub>2</sub>O flux measurements in temperate floodplain forests have been reported yet. Therefore, it remains uncertain if stem surfaces contribute significantly to the N<sub>2</sub>O exchange in these ecosystems.

There are many open questions regarding the mechanisms controlling the GHG exchange at the bark-atmosphere interface. Studies have demonstrated that tree stems essentially act as a pathway of (deeper layer) soil formed CH<sub>4</sub> to the atmosphere (Pangala et al. 2017). This happens either via the transpiration stream or via air-filled aerenchyma

tissues that are morphological adaptations to wetland conditions (e.g. in black alder stems) and serve inter alia to aerate the root system in case of flooding (Rusch and Renneberg 1998). The gas transport within the tree occurs via diffusion or is additionally supported by pressurized gas flow (Colmer 2003; Butterbach-Bahl et al. 2011). Acting as transport pathway, the exchange of N<sub>2</sub>O and CH<sub>4</sub> on the stem surfaces likely depends on GHG concentration gradients between the soil, roots, stem and atmosphere (Colmer 2003; Maier et al. 2018). However, recent evidence points out that further mechanisms may account for the GHG exchange of tree stems (Covey et al. 2012; Lenhart et al. 2018; Covey and Megonigal 2019). The occurrence of methanogenic microbes in the heartwood could lead to the in-situ production of CH<sub>4</sub> inside the stem (Wang et al. 2016, 2017, Yip et al. 2018). It further has been suggested that CH<sub>4</sub> can also be produced in plant tissues under aerobic conditions (Keppler et al. 2006; Messenger et al. 2009). Similar to CH<sub>4</sub>, still unresolved non-microbial processes inside the plants seem to add to the N<sub>2</sub>O emissions from tree stems (Lenhart et al. 2018). First studies also show that some tree species are capable also of taking up N<sub>2</sub>O and CH<sub>4</sub> from the atmosphere by yet not specified mechanisms (Sundqvist et al. 2012; Machacova et al. 2017, 2019). The uptake of N<sub>2</sub>O was found to be higher in the presence of lichens and mosses at the stems of European beech (*Fagus sylvatica*) (Machacova et al. 2017). The various different release and uptake processes and pathways may therefore lead to substantial radial and vertical variability of stem surface GHG fluxes.

The present study aimed at quantifying CH<sub>4</sub> and N<sub>2</sub>O fluxes from tree stems in a temperate floodplain forest and to determine the role of the main environmental factors controlling these fluxes. We repeatedly measured stem surface CH<sub>4</sub> and N<sub>2</sub>O fluxes along a natural flooding gradient in the Danube National Park, Austria. We hypothesized that: (1) tree stems of *Fraxinus excelsior* and *Populus alba* emit N<sub>2</sub>O and CH<sub>4</sub> at measurable quantities, (2) stem GHG emissions at the frequently-flooded site are higher than at the infrequently-flooded and non-flooded site and that (3) CH<sub>4</sub> efflux significantly increases during and after flooding. Finally, we hypothesize that (4) stem GHG fluxes varied with tree species and the position (stem height, radial orientation) of the measurement chambers.

## Materials and methods

### Study sites

The study was conducted in the Danube National Park in Austria, which is situated between Vienna and Bratislava, covering ~10,000 ha along the Danube river. The national park's land-cover consists of 65% forests, 15% meadows and 20% water bodies and has a long history of land use, including water regulation, logging and agriculture (Nationalpark Donau-Auen GmbH 2018). Along the national park, the Danube river has the character of an alpine stream. River discharge ranges from 600 to 900 m<sup>3</sup> sec<sup>-1</sup> at low flow to 8500–11,000 m<sup>3</sup> sec<sup>-1</sup> in the event of a 100-year flood, causing fluctuations of the water table as much as seven meters in height. The mean annual temperature (between 1981 and 2010), measured at the close by meteorological station of Groß-Enzersdorf, was 10.3 °C. The mean precipitation during the same period was 516 mm with a peak during spring and summertime (ZAMG 2020).

Three study sites were selected in a forested national park section near the village of Stopfenreuth (48°08' 39.7"N 16°53'03.7"E). The sites were selected along a ~1 km long transect, consisting of a non-flooded site beyond the Marchfeld-dike (146.8 m a.s.l.), a infrequently-flooded site within the dike (145.7 m a.s.l.), which was considered to be flooded approximately once every 1–3 years, and a lower laying (439.7 m a.s.l.) frequently (several inundations per year) flooded site close to a disconnected Danube side arm. The three sites are hereafter referred to as “non-flooded; NF”, “infrequently-flooded; IF” and “frequently-

flooded, FF”. FF and IF were dominated by silver poplar (*Populus alba* L.) and NF by common ash (*Fraxinus excelsior* L.) (Table 1). The bark of the trees was in parts populated by the mosses *Platydictya subtilis*, *Brachythecium rutabulum* and *Eurhynchium hians*. Basic stand characteristics (tree species, stem diameter at breast height (DBH), tree height) were estimated at each site within a 10 × 10 m study plot. Tree heights were estimated trigonometrically using Vertex IV and Transponder T3 (Haglöf, Sweden) at trees > 5 cm DBH.

### Environmental parameters

Soil temperature (PT100 thermometer, EMS, Czech Republic) and soil moisture (GS3, Decagon, USA) were measured automatically at different soil depths (0.05, 0.15, 0.30, 0.60, 1.00 m) at a single location at the centre of each site. Temporal resolution was 30 min and data were stored on three dataloggers (EM50, Decagon, USA). In addition, soil temperature (at 0.05 m depth) and moisture (0–0.2 m soil depth) were measured manually during each measurement campaign (stem and soil flux) adjacent to each individual stem with a portable thermometer and a TDR moisture meter (Field-Scout, Spectrum Technologies Inc., USA). Precipitation and air temperatures were obtained from the ZAMG weather station Groß-Enzersdorf. Soil moisture was transformed for further calculations into “water filled pore space” (WFPS), a measure that better reflects water saturation of the soil matrix. This measure expresses the ratio of soil volumetric water content (VWC) to total soil porosity and is calculated as:

**Table 1** Site characteristics and tree biometric parameters at the study sites with soil type classified according to WRB (World reference base on soils) IUSS Working Group WRB (2015) and tree species proportions calculated according to site inventory

Site	Non-flooded	Infrequently-flooded	Frequently-flooded
Soil Type	Calcaric Fluvisol	Calcaric Fluvisol	Calcaric Endogleyic Fluvisol
Tree species [%BA]	<i>Fraxinus. excelsior</i> [99] <i>Juglans regia</i> [1]	<i>Populus. alba</i> [90] <i>Ulmus minor</i> [10]	<i>Populus alba</i> [100]
BA (m <sup>2</sup> ha <sup>-1</sup> )	46	55	96
N (n ha <sup>-1</sup> )	700	500	800
V (m <sup>3</sup> ha <sup>-1</sup> )	521	715	865
DBH (m)	0.26 ± 0.13	0.34 ± 0.16	0.36 ± 0.14
Tree height (m)	18.8 ± 8.1	27.2 ± 6.9	23.6 ± 5.2

BA, basal area; N, stem number; V, volume; DBH, tree stem diameter 1.3 m above ground

Values are mean ± 1 SD,  $n_{\text{non-flooded}} = 11$ ;  $n_{\text{infrequently-flooded}} = 13$ ;  $n_{\text{flooded}} = 11$

$$WFPS = VWC \div \left( 1 - \left( \frac{BD}{PD} \right) \right)$$

whereby porosity (BD/Pd) is derived from the bulk density (BD; 0.97 g soil cm<sup>-3</sup>) and particle density (PD; 2.65 g soil cm<sup>-3</sup>).

#### Stem GHG flux measurements

Stem GHG flux measurements were conducted every three weeks from April 2018 to March 2019, making a total of 16 measurement campaigns. An additional intensive measurement campaign was performed during a flooding event in March 2019. All stem chambers were installed two weeks prior to the first measurement campaign ( $n = 84$ ). At each of the three study sites, six randomly chosen trees were equipped with a set of two chambers each at 0.30 and 1.6 m stem height, placed on opposing sides of the stem to account for possible radial flux heterogeneity. Additional chamber sets were mounted at 3.60 m stem height at NF and FF. DBH of poplar trees ranged from 0.21 to 0.63 m whereas DBH of ash trees ranged from 0.34 to 0.71 m.

The stem chambers were built according to Machacova and others (Machacova et al. 2017) out of transparent plastic (polypropylen) storage boxes with removable airtight lids (Lock&Lock, Anaheim, USA). The bottoms of the boxes were cut out and the thereby generated edge was glued to a 2 cm thick neoprene frame. This frame allowed, after smoothing of the tree bark, the airtight gluing on the tree stems using assembly adhesive (Fix ALL TURBO MS-Polymer, Soudal, Turnhout, Belgium). Each chamber lid was equipped with a rubber septum. Chamber lids were attached to the chambers only during flux measurements. We added an additional second septum, equipped with a syringe needle, to assure pressure equilibrium during gas sampling. The volume of the chambers was 0.00196 m<sup>3</sup> ( $h = 0.07$  m, area = 0.018 m<sup>2</sup>) (Machacova et al. 2017).

During each measurement campaign, all chambers were measured on the same day in random order to avoid the effects of diurnal flux fluctuations. Chambers served as closed static systems. Four gas samples were taken every half hour after chamber closure (0–0.5–1.0–1.5 h). The optimal closing time was determined during pre-experimental tests. From each chamber, gas samples of 12 ml were injected into pre-evacuated 10 ml glass vials to achieve a slight overpressure during sample

storage. During about two thirds of the measurement campaigns, we took mixed samples (2 × 6 ml) from the two opposite chambers at the same stem height. To assess the effects of radial variability and potential effects of the presence of mosses, all individual chambers were sampled separately in April, August, and November 2018, and February 2019.

The gas samples were analysed with a gas chromatography (GC) (AGILENT 6890 N, CA, USA) equipped with a <sup>63</sup>Ni-electron-capture detector (ECD) for N<sub>2</sub>O and a flame ionization detector (FID) for CO<sub>2</sub> and CH<sub>4</sub>. Argon was used as a carrier gas for ECD with a flow rate of 9 ml min<sup>-1</sup>, while Helium served as the carrier gas for the FID (flow rate: 15 ml min<sup>-1</sup>). Calibration was performed using 251, 515 and 991 ppm CO<sub>2</sub>, 1.11, 2.11 and 3.98 ppm CH<sub>4</sub> and 1.02, 1.95 and 4.05 ppm N<sub>2</sub>O.

In an accompanying experiment (Schindlbacher et al. in preparation), soil CH<sub>4</sub> and N<sub>2</sub>O fluxes were measured during the same days as stem fluxes. Static soil chambers (diameter 0.30 m, height 0.10 m) were randomly installed at six plots at each site, at a maximum distance of 2 m away from tree stems, which were closed and sampled for 20 min (0, 5, 10, 20, min). Gas samples and GHG fluxes were analysed and calculated as described above. The GHG concentration in the soil air was measured by gas sampling from stainless-steel capillaries installed at 0.10, 0.20, 0.30, 0.50, and 1.00 m soil depth at a single position in the centre of each site.

#### Flux calculation and extrapolation

Stem surface gas fluxes were calculated as:

$$F_c = (\Delta c/t) * (V/A)$$

$F_c$  being the stem surface flux, derived by the rate of linear concentration change over the given time ( $\Delta c/t$ ) within the chambers volume ( $V$ ) via the area of the emitting surface ( $A$ ) and expressed as  $\mu\text{g CH}_4\text{-C m}^{-2}\text{ h}^{-1}$  and  $\mu\text{g N}_2\text{O-N m}^{-2}\text{ h}^{-1}$ . The criteria for a valid single flux measurement being distinguished from zero was an  $R^2 > 0.7$  (Welch et al. 2019) and a value above the detection limit of  $\pm 2.63 \mu\text{g CH}_4\text{-C m}^{-2}\text{ h}^{-1}$  (3 data points) and  $\pm 2.52 \mu\text{g CH}_4\text{-C m}^{-2}\text{ h}^{-1}$  (4 data points), and of  $\pm 0.55 \mu\text{g N}_2\text{O-N m}^{-2}\text{ h}^{-1}$  and  $\pm 0.53 \mu\text{g N}_2\text{O-N m}^{-2}\text{ h}^{-1}$ , respectively (Parkin et al. 2012). Chamber data with  $R^2 < 0.7$  and smaller values than the limit of detection (LOD) were visually checked and zero flux

was assigned if the regression line was horizontal. Fluxes were expelled if the gas concentrations featured a randomly fluctuating pattern in the visual observation. Therefore 49 CH<sub>4</sub> and 63 N<sub>2</sub>O fluxes (out of 673 per gas) were expelled.

For the calculation of the annual sum per hectare, the hourly stem fluxes were up-scaled using the data obtained from the forest inventory. In detail, two steps were performed. First, the geometrically complex tree trunk shapes of the forest inventory were simplified to cylindrical lateral surfaces (Díaz-Pinés et al. 2016). The up-scaling was performed up to the tree height best covered by our chamber measurements. This part was divided into three segments corresponding to the three GHG measurement heights. For each segment, the stem surface was approximated by a cylindrical surface whose diameter and height depends on the chamber position (bottom: 0–0.60 m, middle: 0.60–2.00 m, top: 2.00–4.60 m). The unequal segment size is due to the fact that each pair of chambers represents the flux of the surrounding bark surface at different heights along the stem. These cylindrical segments multiplied by the inventory data (stem number and stem diameter distribution) gives the stem surface from 0 to 4.6 m stem height per hectare forest soil. In a second step, the mean flux rates per sampling, stem segment, and site were extrapolated to annual sums. In order to take the different intervals between the samplings into account, the mean fluxes of a sampling were multiplied by the days until the next sampling.

### Statistical analysis

Since the normality assumptions for parametric tests were not met, we used a Kruskal-Wallis test to verify the differences in stem GHG fluxes between the three study sites. Therefore, an annual mean value was calculated for each chamber. This resulted in six ( $n = 6$ ) and three ( $n = 3$ ) replicates per site and stem measurement height, respectively. The site differences were tested separately for each stem measurement height. A Bonferroni corrected Dunn-test was performed as a post-hoc test.

A t-test was carried out to investigate whether mosses growing on the tree stems significantly affect stem flux. Therefore, we tested 9 pairs of opposing chambers (one chamber with, the other one without moss cover). A significant positive or negative difference from zero

would have indicated an effect from the presence of mosses.

Linear mixed effects models from the lme4 package of the R statistics program (Bates et al. 2015), were used separately for CH<sub>4</sub> and N<sub>2</sub>O to determine the correlations between soil temperature, WFPS, soil and stem flux. Linear regressions of the same package were performed to assess the flux rates with respect to stem height. All statistical analysis was performed with R v.3.1.2 (R core team 2017). Figures were generated using the package ggplot 2 package (Wickham 2009) and Sigma Plot v14.0 (Systat Software Inc., USA).

The data that support the findings of this study are openly available in “figshare” at <http://doi.org/10.6084/m9.figshare.12173856>.

## Results

### Site and soil microclimate

Mean air temperature and total precipitation during the investigation period were 13.0 °C and 851 mm, respectively (Fig. 1), which is 2.7 °C higher and 335 mm more than the 1981–2010 climatic mean measured at the same weather station (ZAMG 2020). WFPS was generally highest at FF, followed by IF and NF (Fig. 1). NF and IF were not flooded during the study period. FF was inundated during June 14–15 and June 29 of 2018, and during March 16–18 of 2019. Water table at FF was close to the soil surface (0 to –1 m depending on the tree location) from April 2018 until July 2018 but dropped below one to two metres during the dry summer/autumn (July–October) of 2018. During autumn/winter 2018 and spring 2019, the groundwater level was again close to the soil surface at FF (Schindlbacher, unpublished data). Groundwater tables at NF and IF lay always more than three meters below the soil surface.

### Site specific CH<sub>4</sub> fluxes

Mean CH<sub>4</sub> fluxes across all stem measurement dates and heights were (mean ± standard error) 2.51 ± 12.71 (NF), 5.2 ± 17.26 (IF), and 11.15 ± 24.04 μg CH<sub>4</sub> C m<sup>-2</sup> h<sup>-1</sup> (FF). Stem CH<sub>4</sub> fluxes showed high temporal and spatial variability throughout the study (Fig. 2a–c), ranging between –46.64 to 57.86 (NF), –58.68 to 92.07 (IF) and –55.78 to 162.89 μg CH<sub>4</sub> C m<sup>-2</sup> h<sup>-1</sup> (FF). With regard

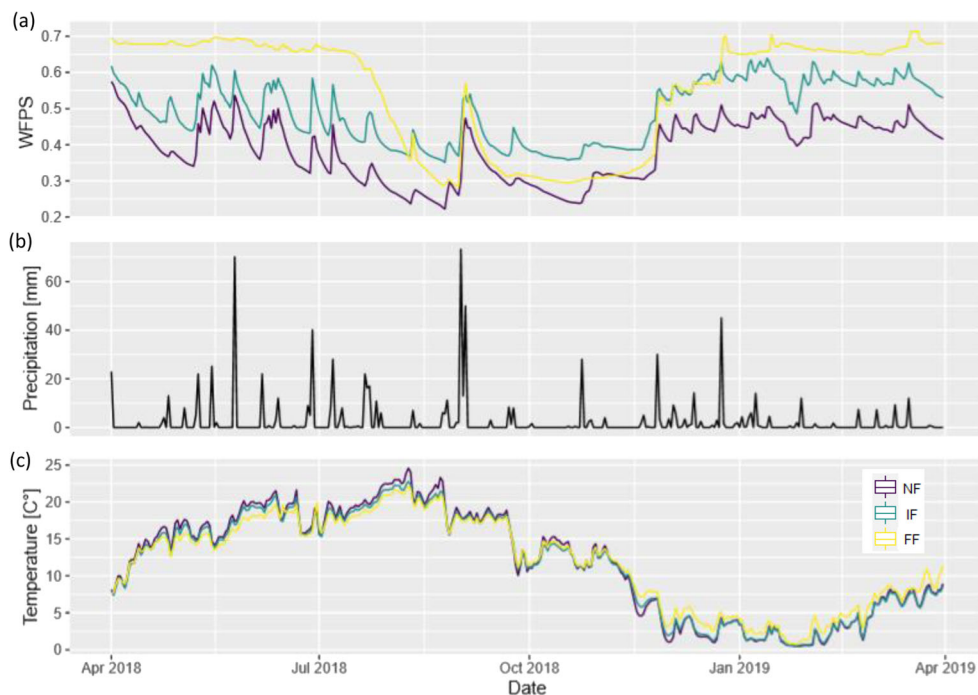


**Fig. 1** Water filled pore space (WFPS) (a), daily mean precipitation (mm) (b) and soil temperature ( $^{\circ}\text{C}$ ) (c) at the three observed sites (non-flooded, purple; infrequently-flooded, turquoise;

frequently-flooded, yellow) along a natural gradient at Danube National Park between April 2018 and April 2019

to the specific measurement height, stem base (0.3 m)  $\text{CH}_4$  fluxes at NF ( $0.18 \pm 0.86 \mu\text{g CH}_4 \text{ C m}^{-2} \text{ h}^{-1}$ ) were significantly below fluxes at IF ( $9.02 \pm 2.95 \mu\text{g CH}_4 \text{ C m}^{-2} \text{ h}^{-1}$ ,  $p = 0.0386$ ) and FF ( $16.25 \pm 7.51 \mu\text{g CH}_4 \text{ C m}^{-2} \text{ h}^{-1}$ ,  $p = 0.0074$ ) but there was no difference between  $\text{CH}_4$  fluxes at IF and FF. At a stem-height of 1.60 m average  $\text{CH}_4$  fluxes at different sites did not differ from each other ( $p = 0.2291$ ). At a stem-height of 3.60 m,  $\text{CH}_4$  fluxes at NF were significantly ( $p = 0.049$ ) higher ( $5.62 \pm 1.56 \mu\text{g CH}_4 \text{ C m}^{-2} \text{ h}^{-1}$ ) than at FF ( $-0.23 \pm 0.93 \mu\text{g CH}_4 \text{ C m}^{-2} \text{ h}^{-1}$ ). Overall, no clear seasonal trend - except a significant difference ( $p=0.0217$ ) between summer and autumn flux at the lowest measurement height at IF - was observed.

#### Site specific $\text{N}_2\text{O}$ fluxes

Stem  $\text{N}_2\text{O}$  fluxes were overall low and highly variable (Fig. 2d-f), ranging between  $-11.87$  to  $30.28$  (NF),  $-12.59$  to  $13.48$  (IF) and  $-68.33$  to  $21.19 \mu\text{g N}_2\text{O N m}^{-2} \text{ h}^{-1}$  (FF). We observed a significant lower  $\text{N}_2\text{O}$  flux during spring than during summer ( $p=0.0300$ ) and winter ( $p=0.0322$ ) at 0.3 m stem height at IF. Higher fluxes in summer, in comparison to autumn ( $p=0.0326$ ) and winter ( $p=0.0329$ ), were

observed at IF, also at the lowest measurement height. NF showed significantly higher fluxes during wintertime at a stem height of 1.60 m in comparison to spring ( $p=0.0301$ ) and autumn ( $p=0.0165$ ). Mean  $\text{N}_2\text{O}$  fluxes across all sampling dates and stem measurement heights were  $1.57 \pm 4.02$  (NF),  $1.35 \pm 3.8$  (IF) and  $0.87 \pm 5.98 \mu\text{g N}_2\text{O N m}^{-2} \text{ h}^{-1}$  (FF). Significant site differences in stem  $\text{N}_2\text{O}$  fluxes could only be found between the 3.60 m chambers of NF and IF ( $1.96 \pm 0.27$  and  $0.03 \pm 0.05 \mu\text{g N}_2\text{O N m}^{-2} \text{ h}^{-1}$ ,  $p=0.049$ ). Mean  $\text{N}_2\text{O}$  fluxes at the stem base ( $p=0.8844$ ) and at 1.6 m did not differ between sites ( $p=0.8054$ ).

#### Environmental drivers

The linear mixed effects model showed that WFPS and soil temperature correlated positively with  $\text{CH}_4$  stem fluxes at all three sites. Soil air  $\text{CH}_4$  concentrations and soil  $\text{CH}_4$  fluxes showed no correlation with stem  $\text{CH}_4$  fluxes (Table 2). Stem  $\text{N}_2\text{O}$  fluxes correlated positively with soil  $\text{N}_2\text{O}$  fluxes. Air temperature and soil air  $\text{N}_2\text{O}$  concentrations showed no significant relationship with stem  $\text{N}_2\text{O}$  fluxes (Table 2). Inundation of FF in March 2019 did not result in any significant immanent increase in stem surface  $\text{CH}_4$  or  $\text{N}_2\text{O}$  fluxes during or after flooding (Fig. S1).

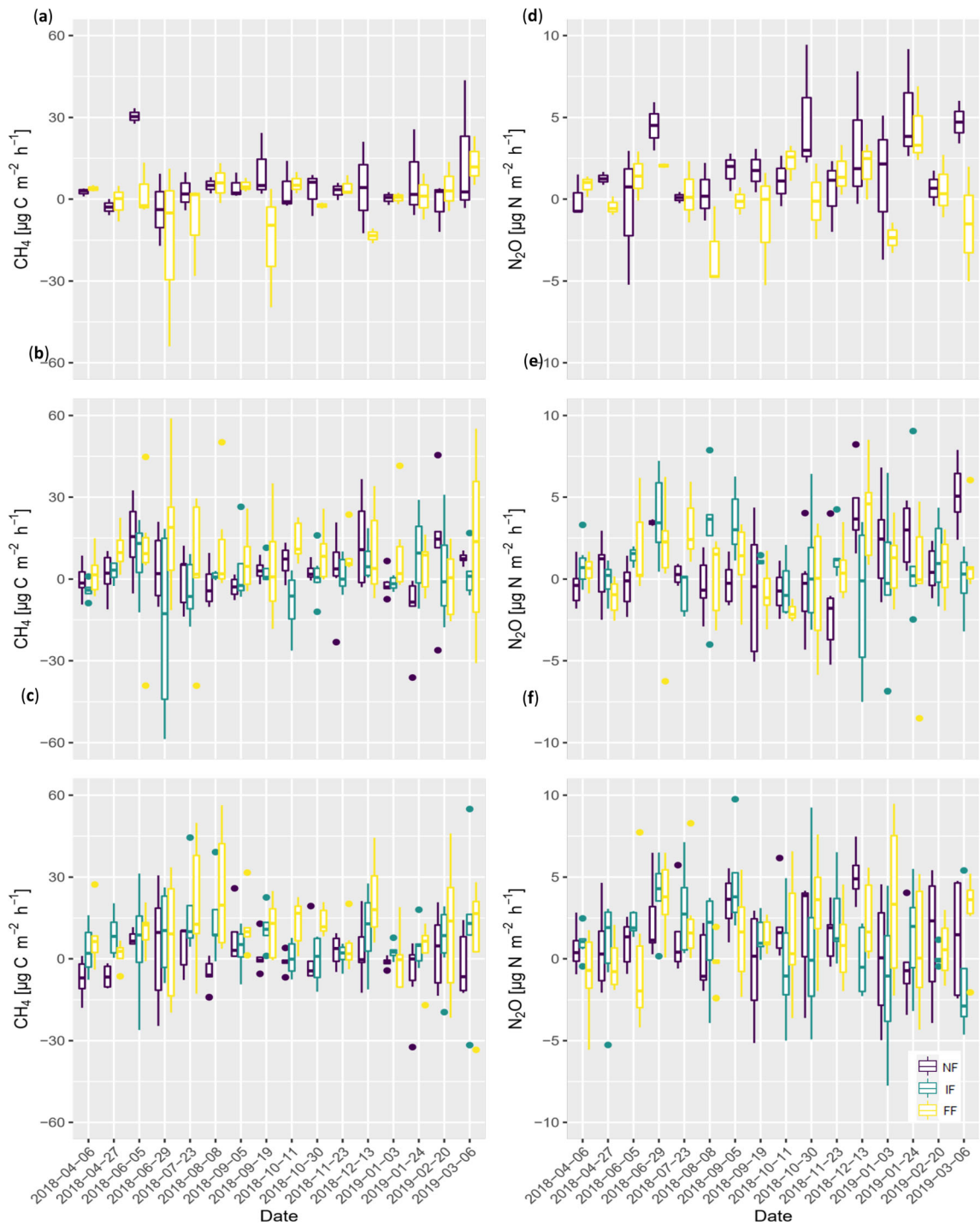


**Fig. 2** CH<sub>4</sub> and N<sub>2</sub>O stem fluxes at the measured sites (non-flooded, purple; infrequently-flooded, turquoise; frequently-flooded, yellow) and at measurement heights of 3.6 m (a, d), 1.6 m (b, e) and 0.3 m (c, f) above the soil surface. Box plots are

due to replication per tree height ( $n_{0.3\text{m}}=6$ ;  $n_{1.6\text{m}}=6$ ;  $n_{3.6\text{m}}=3$ ). Solid line inside the boxplots marks the mean. Dots are values outside the whiskers (1.5 times the inter quartile range)

**Table 2** Summary statistics for the best linear mixed effects models fitted to stem-base (0.3 m) N<sub>2</sub>O ( $\mu\text{g N}_2\text{O N m}^{-2} \text{h}^{-1}$ ) and CH<sub>4</sub> ( $\mu\text{g CH}_4 \text{ C m}^{-2} \text{h}^{-1}$ ) fluxes with the fixed effects of soil N<sub>2</sub>O

( $\mu\text{g N}_2\text{O N m}^{-2} \text{h}^{-1}$ ) and CH<sub>4</sub> ( $\mu\text{g CH}_4 \text{ C m}^{-2} \text{h}^{-1}$ ) flux, soil N<sub>2</sub>O and CH<sub>4</sub> concentrations (ppm), water filled pore space (WFPS) and soil temperature ( $^{\circ}\text{C}$ )

Model	Variables	Value	Std. Error	t-value	<i>p</i> value
Stem CH <sub>4</sub> flux	(Intercept)	-14.118	7.529	-1.875	0.076
	Soil CH <sub>4</sub> flux	-0.002	0.071	-0.022	0.983
	WFPS	0.340	0.099	3.426	<b>0.003</b>
	Soil temp (0.5 m)	0.463	0.198	2.34	<b>0.030</b>
	Soil air CH <sub>4</sub> concentration (0.5 m)	-0.014	0.023	-0.523	0.607
Stem N <sub>2</sub> O flux	(Intercept)	1.797	3.045	0.590	0.560
	Soil N <sub>2</sub> O flux	0.324	0.127	2.544	<b>0.018</b>
	WFPS	-0.036	0.022	-1.605	0.121
	Soil temp (0.5 m)	-0.039	0.083	-0.467	0.645
	Soil air N <sub>2</sub> O concentration (0.5 m)	2.205	5.233	0.421	0.677

Measurement day was included as a random effect.  $n = 45$

Statistically significant values are indicated in bold text

### Tree species specific stem GHG flux patterns

*Populus alba* and *Fraxinus excelsior* showed different GHG flux patterns along the vertical stem axis (Fig. 3). CH<sub>4</sub> and N<sub>2</sub>O fluxes measured from poplar trees decreased significantly ( $-1.42 \pm 0.33 \mu\text{g CH}_4 \text{ C m}^{-1} \text{h}^{-1}$ ,  $p < 0.001$ ) with increasing stem measurement height. Ash trees showed an opposite pattern - increasing CH<sub>4</sub> fluxes with increasing height ( $1.72 \pm 0.67 \mu\text{g CH}_4 \text{ C m}^{-1} \text{h}^{-1}$ ;  $p = 0.011$ ). For N<sub>2</sub>O, no relationship was found with measurement height.

Radial variability of stem fluxes (expressed as standard deviation between the opposing chambers per stem height) was not dependent on measurement-height, site or tree species. Opposing chambers sometimes showed

even uptake and efflux at the same time. Therefore, standard deviation between opposing chambers on individual stems ranged from  $\pm 0.04$  to  $\pm 61.65 \mu\text{g CH}_4 \text{ C m}^{-2} \text{h}^{-1}$  for CH<sub>4</sub> and  $\pm 0.01$  to  $\pm 13.20 \mu\text{g N}_2\text{O N m}^{-2} \text{h}^{-1}$  for N<sub>2</sub>O for poplar and from  $\pm 0.06$  to  $\pm 44.84 \mu\text{g CH}_4 \text{ C m}^{-2} \text{h}^{-1}$  for CH<sub>4</sub> and  $\pm 0.05$  to  $\pm 8.97 \mu\text{g N}_2\text{O N m}^{-2} \text{h}^{-1}$  for ash. The abundance of moss cover did not explain the observed radial and vertical variations in N<sub>2</sub>O and CH<sub>4</sub> fluxes (Fig. S2).

### Up-scale of stem GHG fluxes to site level

The extrapolation of the tree stem fluxes to the forest ground areas resulted in the highest CH<sub>4</sub> stem emissions at FF. Soils acted overall as sinks for CH<sub>4</sub>, while their

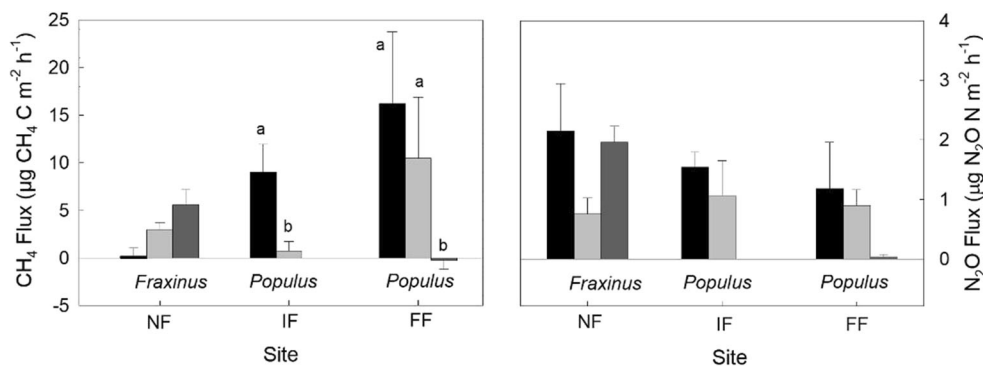


**Fig. 3** Mean annual CH<sub>4</sub> (left) and N<sub>2</sub>O (right) stem surface fluxes at the three observed sites (non-flooded, NF; infrequently-flooded, IF; frequently-flooded, FF) at the three measurement heights of 0.3 m (black bars), 1.6 m (light grey bars) and 3.6 m

(dark grey bars) above ground.  $n_{0.3\text{m}}=6$ ;  $n_{1.6\text{m}}=6$ ;  $n_{3.6\text{m}}=3$ . Error bars indicate SD. Statistically significant differences ( $p < 0.05$ ) in fluxes between measurement heights of the same site are indicated by different letters above the bars



sink strength decreased towards the wetter (flooded) sites (Table 3). Tree stems offset the CH<sub>4</sub> sink strength of the soil by 1.2% (NF), 1.1% (IF) and 30% (FF). N<sub>2</sub>O emissions from tree stems were similar across all sites and accounted for 5.1% (FF), 3.1% (IF) and 7.4% (NF) of soil emissions (Table 3).

## Discussion

To our knowledge, we show here for the first time that white poplar (*Populus alba*) and common ash (*Fraxinus excelsior*) can emit significant quantities of N<sub>2</sub>O and CH<sub>4</sub> from their stem surfaces to the atmosphere. Therefore, they offer additional surface area (in our case roughly in similar size than the soil surface) for GHG exchange in the forest ecosystem. Accordingly, when taken into account, stem GHG fluxes can improve forest ecosystem GHG budgeting.

The studied stems in the floodplain forest were net sources of CH<sub>4</sub> at the non-flooded site ( $2.51 \pm 12.71$ ), the infrequently-flooded site ( $5.2 \pm 17.26$ ) and the frequently-flooded site ( $11.15 \pm 24.04 \mu\text{g CH}_4 \text{ C m}^{-2} \text{ h}^{-1}$ ). These overall moderate stem GHG emissions are rather comparable to those from temperate upland forests (Pitz & Megonigal 2017; Warner et al. 2017; Maier et al. 2018; Barba et al. 2019) and lower than stem CH<sub>4</sub> emissions from waterlogged temperate wetland ecosystems. Methane stem emissions from temperate forested wetlands were found to range between  $101 \mu\text{g CH}_4 \text{ C m}^{-2} \text{ h}^{-1}$  from mature alder trees (Gauci et al. 2010) and  $190 \pm 123 \mu\text{g CH}_4 \text{ C m}^{-2} \text{ h}^{-1}$  from the nine most common wetland tree species of Maryland, USA (Pitz et al. 2018). A study conducted in a temperate floodplain forest on stems of *Fraxinus mandshurica* (Northern Japan) found even higher stem CH<sub>4</sub> emissions, reaching up to  $1492 \mu\text{g CH}_4 \text{ C m}^{-2} \text{ h}^{-1}$ . An explanation for the comparably low stem CH<sub>4</sub> emissions in our study could be the site characteristics of Danube

National Park, which accommodates overall well-draining soils, in combination with the short inundation times (1–3 days), both inhibiting longer periods of anaerobic conditions necessary for relevant CH<sub>4</sub> production in soils.

Methane fluxes showed a positive correlation with WFPS, which was also shown by Barba and others (Barba et al. 2019) on a hickory tree at the St. Jones Estuarine Reserve (Delaware, USA), and by Machacova and others (Machacova et al. 2016) on pine trees in a boreal forest. Stem CH<sub>4</sub> flux also showed a positive correlation with soil temperature, which is a general finding of many authors (Pangala et al. 2015; Wang et al. 2017; Pitz et al. 2018; Barba et al. 2019). No correlations between stem CH<sub>4</sub> efflux, soil CH<sub>4</sub> concentrations and soil CH<sub>4</sub> flux could be found, though significantly higher soil CH<sub>4</sub> concentrations were observed at the generally wetter frequently-flooded site (Fig. S3). The missing correlation could be due to a temporal and spatial mismatch of CH<sub>4</sub> production in the soil and transport into the stem. Methane concentrations in the subsoil were often enhanced during the cold months, which typically are periods of low or ceased tree transpiration. However, diffusion shall have occurred since soil CH<sub>4</sub> concentrations were several ppm higher in the subsoil than in the atmosphere (Covey and Megonigal 2019). Therefore, the low stem efflux possibly is a matter of CH<sub>4</sub> re-consumption in overlaying aerated soil layers or during the transport through the root/stem/bark (Maier et al. 2018). It also has to be noted that soil GHG concentrations were measured at only a single location (soil profile) at each site. Accordingly, our soil GHG concentration profile applied only for a minimal area of the full rooting zone of the six trees. Furthermore, stems were shown to emit CH<sub>4</sub> originating from various sources (Keppler et al. 2006), which leaves the possibility that primarily CH<sub>4</sub> produced within the stem had added to the observed stem surface fluxes.

**Table 3** Comparison of up-scaled annual mean CH<sub>4</sub> (kg CH<sub>4</sub> C ha<sup>-1</sup> yr<sup>-1</sup>) and N<sub>2</sub>O (kg N<sub>2</sub>O N ha<sup>-1</sup> yr<sup>-1</sup>) stem and soil fluxes

	CH <sub>4</sub> flux		N <sub>2</sub> O flux	
	Soil	Stem	Soil	Stem
non-flooded	$-5.11 \pm 0.72$	$0.06 \pm 0.07$	$0.27 \pm 0.08$	$0.02 \pm 0.02$
infrequently-flooded	$-2.85 \pm 0.76$	$0.03 \pm 0.05$	$0.32 \pm 0.06$	$0.01 \pm 0.02$
flooded	$-0.83 \pm 1.02$	$0.25 \pm 0.42$	$0.39 \pm 0.21$	$0.02 \pm 0.02$

Values are mean  $\pm$  1 SD

In contrast to other studies, stem CH<sub>4</sub> fluxes did not show a distinctive seasonal trend (Pangala et al. 2015; Barba et al. 2019). The slight increase of stem CH<sub>4</sub> flux during the summer, however, was explained by the overall positive correlation between soil temperature and stem CH<sub>4</sub> flux.

Contrary to our hypotheses, we did not observe any imminent effects of flooding/inundation on stem CH<sub>4</sub> fluxes during the flooding event between March 17th - 19th. The likely most significant reason was the short inundation time of 1–3 days. In the studied ecosystem floods retreat from most of the forested floodplain areas within days to weeks, which stands in sharp contrast to other forested wetlands, which are typically water-logged for weeks or months. Accordingly, inundation times were likely not long enough to create and maintain anaerobic conditions that allow for the growth of a methanogenic microbial population and significant CH<sub>4</sub> production (Machacova et al. 2013). That the soil pore-water CH<sub>4</sub> concentrations did not significantly increase after flooding (data not shown) supports this explanation. Since all floods during our study were of minor magnitude, it remains open if more severe flooding and longer inundation periods could cause a significant increase in stem CH<sub>4</sub> efflux. However, severe floods with longer inundation times occur only in decadal or centurial intervals and the quantitative effects on CH<sub>4</sub> emissions would therefore be limited in this floodplain forest.

Stems were net sources of N<sub>2</sub>O on the non-flooded site ( $1.57 \pm 4.02$ ), the infrequently-flooded site ( $1.35 \pm 3.8$ ) and on the frequently-flooded poplar ( $0.87 \pm 5.98 \mu\text{g N}_2\text{O N m}^{-2} \text{h}^{-1}$ ). These values are in a similar range as observations from temperate upland forests (Díaz-Pinés et al. 2016; Wen et al. 2017). In some non-flooded forests, N<sub>2</sub>O uptake was observed at stem surfaces (Machacova et al. 2017; Barba et al. 2019), which was also periodically observed in our study. We observed higher N<sub>2</sub>O fluxes from the infrequently-flooded site during summer, which is in line with results in a boreal forest by Machacova and others (Machacova et al. 2019), who linked the tree physiological activity to stem N<sub>2</sub>O emissions. We further observed higher N<sub>2</sub>O fluxes during wintertime at the non-flooded site, which could be connected to specific responses of the ash trees to freezing events (Machacova et al. 2019). However, this remains speculative and further research is needed to find the reason for the distinct occurrence of these seasonal differences at the differently located sites.

Stem N<sub>2</sub>O fluxes of the lowest laying chambers correlated with soil N<sub>2</sub>O flux, which was also observed by others (Machacova et al. 2013, 2019; Barba et al. 2019), suggesting that the N<sub>2</sub>O emissions measured from the stem surface originate from the soil. The flooding events during our study had no significant impact on N<sub>2</sub>O stem fluxes as well. This was expected, since totally anaerobic conditions favour the production of N<sub>2</sub> over N<sub>2</sub>O during denitrification processes.

The most striking observation in our study was that the two tree species showed an inverse GHG efflux pattern along the vertical stem axis. Poplar showed a sharp decrease in CH<sub>4</sub> as well as N<sub>2</sub>O effluxes with increasing stem measurement height, whereas ash showed a gradual increase in CH<sub>4</sub> emissions with increasing stem measurement height and a random N<sub>2</sub>O flux pattern. Most previous studies showed a general decline in CH<sub>4</sub> and/or N<sub>2</sub>O emission with increasing stem measurement height. Such a trend was observed for several tropical tree species (Pangala et al. 2013), *Fraxinus mandshurica* (Terazawa et al. 2007), *Alnus glutinosa* and *Betula pubescens* (Pangala et al. 2015), *Fraxinus augustifolia* and *Fagus sylvatica* (Díaz-Pinés et al. 2016), and *Alnus incana* (Schindler et al. 2020). To our knowledge, there is only one other study (Maier et al. 2018) that reported increasing CH<sub>4</sub> emissions with stem measurement height. Maier et al. (2018) detected similar flux patterns as those of the ash stems in our study on *Fagus sylvatica* stems, which served as high CH<sub>4</sub> emitters (Maier et al. 2018), but the underlying mechanisms that caused the increasing CH<sub>4</sub> efflux from the stem base up to two meters height remained unresolved in their study. While decreasing efflux rates with stem height are consistent with the “pathway-theory”, which suggests stems as conduits for GHGs produced in the soil (Pitz and Megonigal 2017), other CH<sub>4</sub> forming processes have been suggested to contribute directly to stem surface fluxes (Covey et al. 2012; Wang et al. 2016; Barba et al. 2019; Yip et al. 2018). The highest CH<sub>4</sub> emissions from ash - detected at a stem height of 3.6 m could therefore be associated with the existence of methanogenic microbes within the stem (Covey et al. 2012; Yip et al. 2018). Ash is known for its facultative heartwood formation, which also could be observed at the studied trees. It has been shown that the heartwood has the highest water contents in ash stems (Kerr 1998), at least indicating preferential conditions for CH<sub>4</sub> production therein. This, however, remains speculative, as we could not trace the location of CH<sub>4</sub> formation in

trunk wood in our study. Another possible explanation for the increasing CH<sub>4</sub> emissions with stem height could be hollow or moldered trunk parts caused by saprotrophic fungi infestation. Some of the ash trees in the Danube National Park is infested with the fungus *Hymenoscyphus fraxineus*, which causes massive ash die-back in all parts of Austria (Halmschlager and Kirisits 2008). Infested trees are particularly susceptible to saprotrophic fungal attack via the roots (Lenz et al. 2019), which can cause stem-rot. However, increment cores, which were taken from each tree at all GHG measurement heights do not indicate any cavities or rot infestation of any of the studied trees. Regarding the poplar trees, which showed clearly higher emission at the trunk base, the considerably lower wood density ((ÖNORM B 3012) could ease gas diffusion and release most of the soil borne GHG already at the stem base. Another reason of the concentration of fluxes at the trunk base could be aerenchyma tissues, which is also a common physiological feature in ash trees (Glenz et al. 2006).

With regard to the stem GHG flux patterns of ash and poplar, it has to be considered that GHG fluxes from ash stems were exclusively measured at the non-flooded site, whereas those from poplar stems were exclusively measured at the infrequently and frequently-flooded sites. Accordingly, other site factors than tree species cannot be ruled out having influenced the observed GHG efflux patterns. However, the non-flooded and the infrequently-flooded sites lay at almost the same altitude ( $\pm 1$  m) and soils were almost identical in layering and C and N distribution (Schindlbacher et al. in preparation). The only difference between the two sites was that soils at the non-flooded site were slightly dryer. Therefore, we do not see evidence that other effects than tree species accounted for the distinctive vertical stem GHG patterns. Poplar stems at the very contrasting infrequently and frequently-flooded sites showed the same vertical GHG flux patterns, though soil structure, C and N distribution and WFPS differed - further indicating that wood anatomy or other stem specific features rather than other site factors determined the observed GHG flux patterns along the stem axes.

The occurrence of moss cover on the stem surface did not affect the vertical flux patterns in our study. Mosses covering the stem surface were suggested to release or consume CH<sub>4</sub> and N<sub>2</sub>O and thereby influence the stem surface GHG fluxes (Machacova et al. 2017, Lenhart

et al. 2015). Under field-conditions, we found no significant difference between moss-covered and uncovered surfaces. This does not necessarily mean that the moss coverage had no influence on GHG emissions, but shows that, if there was any flux from mosses, it was not detectable in the radial and vertical GHG flux variations.

By measuring stem GHG efflux not only at the stem base but incrementally towards 3.6 m stem height; we identified potential shortfalls in too simplistic flux up-scaling approaches (e.g. by using only a single chamber at the stem base). While, in our study, measurements at a single stem height of e.g. 1.6 m would have indicated similar stem GHG fluxes from ash and poplar, the additional measurements at 0.3 and 3.6 m have shed more light at the, in reality, much more complex stem flux patterns of the two different tree species. Like other authors (Covey and Megonigal 2019), we encourage to incorporate this knowledge in further studies by adding flux measurements even further up the stem. We can also confirm the necessity to tackle radial variability by mounting more than one chamber per height level (Covey et al. 2012; Covey and Megonigal 2019). We applied two chambers at opposing stem surface patches at each measurement height to account for radial variation in GHG fluxes across the stem surface and observed a high radial variability in CH<sub>4</sub> as well as N<sub>2</sub>O fluxes at individual trees. Especially at larger diameter trees, the two chambers covered only a limited portion (< 10%) of the corresponding radial stem surface. Accordingly, our efflux estimates from larger diameter trees hold a higher uncertainty than those from smaller diameter trees. Barba and others (2019 and Jeffrey et al. (2020) highlighted the radial variations of stem GHG fluxes. This variation can be tackled by measuring with multiple chambers or large chambers which cover the full stem circumference (e.g. Siegenthaler et al. 2016, Machacova et al. 2016).

Up-scaling of fluxes to ground area showed that CH<sub>4</sub> emissions from stems could only compensate for a small part of the sink strength of the soils at the dryer sites, whereas roughly a third of the CH<sub>4</sub> soil sink was compensated at the wetter frequently-flooded site. Stem CH<sub>4</sub> emissions compensate only about 1% of the soil uptake at the non-flooded sites (Table 3), which is consistent with the results of Pitz and Megonigal (2017) from temperate deciduous non-flooded forest in Maryland, USA. At our frequently-flooded site, stem emissions offset about 30% of the annual soil CH<sub>4</sub> uptake of the soil. However, due to the wetter site conditions, the CH<sub>4</sub>

soil-sink-strength at the frequently-flooded site was much smaller when compared to the non-flooded and infrequently-flooded sites. Accordingly, the relative effect size of the stem CH<sub>4</sub> emissions was higher at this specific site. With regard to the overall significance of the stem and soil CH<sub>4</sub> fluxes of frequently-flooded forest it has to be noted that such forest only comprise a small (<5%) fraction of the total floodplain forest area.

The low contribution of stem N<sub>2</sub>O fluxes to the total N<sub>2</sub>O fluxes (Table 3) is consistent with other findings from temperate non-flooded soil where similar up-scaling methods were applied (Diaz-Pines et al. 2016; Machacova et al. 2017, 2019). Our extrapolated estimates of stem fluxes are intentionally conservative as we only report fluxes to a maximal height of 4.6 m. We have chosen this conservative approach because the tree-specific height patterns of stem GHG fluxes varied widely. Frequently, flux estimates are extrapolated from a single stem measurement height (usually at the stem base) to the entire stem surface (Machacova et al. 2016; Warner et al. 2017). We have shown that this can massively over- (poplar) or underestimate (ash) the real stem efflux. In fact, we do not know the capacity of stem emissions above 4.6 m in our study. Although it seems plausible that poplars emit significant amounts of CH<sub>4</sub> only at the stem base, we cannot exclude significant stem emissions at stem sections above our highest measured segment (above 4.6 m). On the other hand, it seems plausible that ash trees continue to emit high CH<sub>4</sub> emissions at the stem surface even at stem heights above. If we were to scale up the emissions from the 4.6 m segment to the remaining stem surface up to the tree crown, estimated emissions would approximately triple. Therefore, flux measurements not only at the base of a stem, but further up the stem to the crown would be a necessary step towards a reliable upscaling of the total stem GHG fluxes. For technical/infrastructure reasons, we have not included leaf/shoot gas measurements into our study. However, based on the results of recent studies, (Machacova et al. 2016), leaves could further increase the contribution of trees to CH<sub>4</sub> and N<sub>2</sub>O exchange in the ecosystem.

In summary, we have shown that stems of ash and poplar, widespread tree species in floodplain forests of Central Europe, are annual net emitters of CH<sub>4</sub> and N<sub>2</sub>O. The highest stem emissions of CH<sub>4</sub> were found from poplars growing in moist and periodically flooded soils. The study showed no clear seasonal trends in stem CH<sub>4</sub> and N<sub>2</sub>O fluxes, although water-filled-pore spaces and

soil temperature were identified as environmental controls. The tree species specific flux patterns along the vertical stem axis point to the need for more detailed and highly resolved trace gas measurements up to the crown area in order to better understand the sources and processes behind stem GHG fluxes and to optimise the methods for upscaling GHG fluxes to whole stem and forest stand surfaces.

**Supplementary Information** The online version contains supplementary material available at <https://doi.org/10.1007/s11104-020-04818-4>.

**Acknowledgements** The study was funded by the Austrian Klima- und Energie Fonds (ACRP9 project FloodFlux, KR16AC0K13382) The contributions of Katerina Machacova and Thomas Schindler were supported by the Czech Science Foundation (17-18112Y), the Ministry of Education, Youth and Sports of the Czech Republic within the National Sustainability Program I (grant number LO1415) and the project SustES - Adaptation strategies for sustainable ecosystem services and food security under adverse environmental conditions (CZ.02.1.01/0.0/0.0/16\_019/0000797). We thank Leszek Dariusz Laptaszyński for technical support during chamber installation, Michaela Djordjevic and Armin Hofbauer for support in the GC lab as well as Günther Gollobich and Katarina Stefaner for their support during field work. We thank the national park authorities for their generous support.

**Author contributions** AS designed and planned the research. EM analyzed the data and wrote the first draft of the manuscript. EM and AS performed the measurements. AS, KM, EM installed the stem chambers. BK supervised gas chromatography data management. TS and KM contributed to measurements during the flooding campaign. All authors contributed to the writing of the manuscript.

## References

- Barba J, Bradford MA, Brewer PE et al (2019) Methane emissions from tree stems: a new frontier in the global carbon cycle. *The New phytologist* 222:18–28. <https://doi.org/10.1111/nph.15582>
- Bates D, Mächler M, Bolker B, Walker S (2015) Fitting linear mixed-effects models using lme4. *J Stat Soft* 67. <https://doi.org/10.18637/jss.v067.i01>
- Butterbach-Bahl K, Kiese R, Liu C (2011) Measurements of biosphere-atmosphere exchange of CH<sub>4</sub> in terrestrial ecosystems. *Methods in enzymology* 495:271–287. <https://doi.org/10.1016/B978-0-12-386905-0.00018-8>
- Butterbach-Bahl K, Baggs EM, Dannenmann M et al (2013) Nitrous oxide emissions from soils: how well do we understand the processes and their controls? *Philosophical transactions of the Royal Society of London Series B, Biological*

- sciences 368:20130122. <https://doi.org/10.1098/rstb.2013.0122>
- Colmer TD (2003) Long-distance transport of gases in plants: a perspective on internal aeration and radial oxygen loss from roots. *Plant Cell Environ* 26:17–36. <https://doi.org/10.1046/j.1365-3040.2003.00846.x>
- Covey KR, Megonigal JP (2019) Methane production and emissions in trees and forests. *The New phytologist* 222:35–51. <https://doi.org/10.1111/nph.15624>
- Covey KR, Wood SA, Warren RJ et al (2012) Elevated methane concentrations in trees of a non-flooded forest. *Geophys Res Lett* 39:198. <https://doi.org/10.1029/2012GL052361>
- Díaz-Pinés E, Heras P, Gasche R et al (2016) Nitrous oxide emissions from stems of ash (*Fraxinus angustifolia* Vahl) and European beech (*Fagus sylvatica* L.). *Plant Soil* 398: 35–45. <https://doi.org/10.1007/s11104-015-2629-8>
- Gauci V, Gowing DJG, Hornibrook ERC et al (2010) Woody stem methane emission in mature wetland alder trees. *Atmospheric Environment* 44:2157–2160. <https://doi.org/10.1016/j.atmosenv.2010.02.034>
- Glenz C, Schlaepfer R, Lorgulescu I, Kienast F (2006) Flooding tolerance of Central European tree and shrub species. *Forest Ecology and Management* 235:1–13. <https://doi.org/10.1016/j.foreco.2006.05.065>
- Halmischlager E, Kirisits T (2008) First report of the ash dieback pathogen *Chalara fraxinea* on *Fraxinus excelsior* in Austria. *Plant Pathol* 57:–1177. <https://doi.org/10.1111/j.1365-3059.2008.01924.x>
- IPCC (2013) Summary for Policymakers. In: *Climate Change 2013: The Physical Science Basis. Contribution of Working Group I to the Fifth Assessment Report of the Intergovernmental Panel on Climate Change* [Stocker TF, Qin D, Plattner G-K, Tignor M, Allen SK, Boschung J, Nauels A, Xia Y, Bex V, Midgley PM (eds)]. Cambridge University Press, Cambridge, United Kingdom and New York, NY, USA
- IUSS Working Group WRB (2015) World Reference Base for Soil Resources 2014, update 2015 International soil classification system for naming soils and creating legends for soil maps. In: *World Soil Resources Reports No. 106*. FAO, Rome. Available via <http://www.fao.org/3/i3794en/i3794EN.pdf>. Accessed 9 Nov 2020
- Jeffrey LC, Maher DT, Tait DR, Johnston SG (2020) A small nimble in situ fine-scale flux method for measuring tree stem greenhouse gas emissions and processes (S.N.I.F.F.). *Ecosystems*. <https://doi.org/10.1007/s10021-020-00496-6>
- Kandel TP, Lærke PE, Hoffmann CC, Elsgaard L (2018) Complete annual CO<sub>2</sub>, CH<sub>4</sub>, and N<sub>2</sub>O balance of a temperate riparian wetland 12 years after rewetting. *Ecological Engineering* 127:527–535. <https://doi.org/10.1016/j.ecoleng.2017.12.019>
- Kepler F, Hamilton JTG, Brass M, Röckmann T (2006) Methane emissions from terrestrial plants under aerobic conditions. *Nature* 439:187–191. <https://doi.org/10.1038/nature04420>
- Kerr G (1998) A review of black heart of ash (*Fraxinus excelsior* L.). *Forestry* 71:49–56. <https://doi.org/10.1093/forestry/71.1.49>
- Krause S, Lewandowski J, Grimm NB et al (2017) Ecohydrological interfaces as hot spots of ecosystem processes. *Water Resour Res* 53:6359–6376. <https://doi.org/10.1002/2016WR019516>
- Lenhart K, Weber B, Elbert W et al (2015) Nitrous oxide and methane emissions from cryptogamic covers. *Glob Change Biol* 21:3889–3900. <https://doi.org/10.1111/gcb.12995>
- Lenhart K, Behrendt T, Greiner S, et al (2018) Nitrous oxide effluxes from plants as a potentially important source to the atmosphere. *The New phytologist* 221:1398–1408. <https://doi.org/10.1111/nph.15455>
- Lenz H, Straßer L, Petercord R (2019) Eschentriebsterben: Biologie und Behandlung. In: LWF-Merkblatt 28. Available via [http://www.lwf.bayern.de/mam/cms04/waldschutz/dateien/mb28-eschentriebsterben\\_2019\\_bf.pdf](http://www.lwf.bayern.de/mam/cms04/waldschutz/dateien/mb28-eschentriebsterben_2019_bf.pdf). Accessed 9 Nov 2020
- Machacova K, Papen H, Kreuzwieser J, Rennenberg H (2013) Inundation strongly stimulates nitrous oxide emissions from stems of the non-flooded tree *Fagus sylvatica* and the riparian tree *Alnus glutinosa*. *Plant Soil* 364:287–301. <https://doi.org/10.1007/s11104-012-1359-4>
- Machacova K, Bäck J, Vanhatalo A et al (2016) *Pinus sylvestris* as a missing source of nitrous oxide and methane in boreal forest. *Sci Rep* 6:23410. <https://doi.org/10.1038/srep23410>
- Machacova K, Maier M, Svobodova K et al (2017) Cryptogamic stem covers may contribute to nitrous oxide consumption by mature beech trees. *Sci Rep* 7:13243. <https://doi.org/10.1038/s41598-017-13781-7>
- Machacova K, Vainio E, Urban O, Pihlatie M (2019) Seasonal dynamics of stem N<sub>2</sub>O exchange follow the physiological activity of boreal trees. *Nat Commun* 10:4989. <https://doi.org/10.1038/s41467-019-12976-y>
- Maier M, Machacova K, Lang F et al (2018) Combining soil and tree-stem flux measurements and soil gas profiles to understand CH<sub>4</sub> pathways in *Fagus sylvatica* forests. *Z Pflanzenemähr Bodenk* 181:31–35. <https://doi.org/10.1002/jpln.201600405>
- Messenger DJ, McLeod AR, Fry SC (2009) Reactive oxygen species in aerobic methane formation from vegetation. *Plant Signaling & Behavior* 4:629–630. <https://doi.org/10.4161/psb.4.7.8968>
- Nationalpark Donau-Auen GmbH (2018) Zahlen, Daten, Fakten. In: *Der Nationalpark*. Available via <https://www.donauauen.at/der-nationalpark/zahlen-daten-fakten>. Accessed 28 Feb 2020
- Pangala SR, Moore S, Hornibrook ERC, Gauci V (2013) Trees are major conduits for methane egress from tropical forested wetlands. *The New phytologist* 197:524–531. <https://doi.org/10.1111/nph.12031>
- Pangala SR, Hornibrook ERC, Gowing DJ, Gauci V (2015) The contribution of trees to ecosystem methane emissions in a temperate forested wetland. *Global change biology* 21:2642–2654. <https://doi.org/10.1111/gcb.12891>
- Pangala SR, Enrich-Prast A, Basso LS, et al (2017) Large emissions from floodplain trees close the Amazon methane budget. *Nature* 552:230–234. <https://doi.org/10.1038/nature24639>
- Parkin TB, Venterea RT, Hargreaves SK (2012) Calculating the detection limits of chamber-based soil greenhouse gas flux measurements. *Journal of Environmental Quality* 41:705–715. <https://doi.org/10.2134/jeq2011.0394>
- Pitz S, Megonigal JP (2017) Temperate forest methane sink diminished by tree emissions. *The New phytologist* 214:1432–1439. <https://doi.org/10.1111/nph.14559>

- Pitz SL, Megonigal JP, Chang C-H, Szlavecz K (2018) Methane fluxes from tree stems and soils along a habitat gradient. *Biogeochemistry* 137:307–320. <https://doi.org/10.1007/s10533-017-0400-3>
- R Core Team (2017) R: A language and environment for statistical computing. In: R Foundation for Statistical Computing. Available via <https://www.R-project.org>. Accessed 1 Jan 2020
- Rusch H, Renneberg H (1998) Black alder (*Alnus glutinosa* (L.) Gaertn.) trees mediate methane and nitrous oxide emission from the soil to the atmosphere. *Plant and Soil* 201:1–7. <https://doi.org/10.1023/A:1004331521059>
- Schindler T, Mander Ü, Machacova K, et al (2020) Short-term flooding increases CH<sub>4</sub> and N<sub>2</sub>O emissions from trees in a riparian forest soil-stem continuum. *Sci Rep* 10:3204. <https://doi.org/10.1038/s41598-020-60058-7>
- Shrestha J, Niklaus PA, Frossard E et al (2012) Soil nitrogen dynamics in a river floodplain mosaic. *Journal of environmental quality* 41:2033–2045. <https://doi.org/10.2134/jeq2012.0059>
- Siegenthaler A, Welch B, Pangala SR, et al (2016) Technical Note: Semi-rigid chambers for methane gas flux measurements on tree stems. *Biogeosciences* 13:1197–1207. <https://doi.org/10.5194/bg-13-1197-2016>
- Smith KA, Ball T, Conen F et al (2018) Exchange of greenhouse gases between soil and atmosphere: interactions of soil physical factors and biological processes. *Eur J Soil Sci* 69:10–20. <https://doi.org/10.1111/ejss.12539>
- Sundqvist E, Crill P, Mölder M, Vestin P, Lindroth A (2012) Atmospheric methane removal by boreal plants. *Geophys Res Lett* 39:L21806. <https://doi.org/10.1029/2012GL053592>
- Terazawa K, Ishizuka S, Sakata T, et al (2007) Methane emissions from stems of *Fraxinus mandshurica* var. *japonica* trees in a floodplain forest. *Soil Biology and Biochemistry* 39:2689–2692. <https://doi.org/10.1016/j.soilbio.2007.05.013>
- Tockner K, Stanford JA (2002) Riverine flood plains: present state and future trends. *Envir Conserv* 29:308–330. <https://doi.org/10.1017/S037689290200022X>
- Topp E, Pattey E (1997) Soils as sources and sinks for atmospheric methane. *Can J Soil Sci* 77:167–177. <https://doi.org/10.4141/S96-107>
- Wang Z-P, Gu Q, Deng F-D, et al (2016) Methane emissions from the trunks of living trees on non-flooded soils. *The New phytologist* 211:429–439. <https://doi.org/10.1111/nph.13909>
- Wang Z-P, Han S-J, Li H-L et al (2017) Methane Production Explained Largely by Water Content in the Heartwood of Living Trees in Non-flooded Forests. *J Geophys Res Biogeosci* 122:2479–2489. <https://doi.org/10.1002/2017jg003991>
- Warner DL, Villarreal S, McWilliams K et al (2017) Carbon Dioxide and Methane Fluxes From Tree Stems, Coarse Woody Debris, and Soils in an Non-flooded Temperate Forest. *Ecosystems* 20:1205–1216. <https://doi.org/10.1007/s10021-016-0106-8>
- Welch B, Gauci V, Sayer EJ (2019) Tree stem bases are sources of CH<sub>4</sub> and N<sub>2</sub>O in a tropical forest on non-flooded soil during the dry to wet season transition. *Global Change Biol* 25:361–372. <https://doi.org/10.1111/gcb.14498>
- Wen Y, Corre MD, Rachow C et al (2017) Nitrous oxide emissions from stems of alder, beech and spruce in a temperate forest. *Plant Soil* 420:423–434. <https://doi.org/10.1007/s11104-017-3416-5>
- Wickham H (2009) *Ggplot2: elegant graphics for data analysis*. Springer, New York
- Yip DZ, Veach AM, Yang ZK, et al (2018) Methanogenic Archaea dominate mature heartwood habitats of Eastern Cottonwood (*Populus deltoides*). *The New phytologist* 222: 115–121 <https://doi.org/10.1111/nph.15346>
- Zentralanstalt für Meteorologie und Geodynamik (2020) Klimaforschung. Available via <https://www.zamg.ac.at/cms/de/klima/klimaforschung>. Accessed 28 Feb 2020

**Publisher's note** Springer Nature remains neutral with regard to jurisdictional claims in published maps and institutional affiliations.